


SCIENTIFIC ARTICLE

CircCDR1as Suppresses Bone Microvascular Endothelial Cell Activity and Angiogenesis Through Targeting miR-135b/ FIH-1 Axis

Zheng Mao, MM¹, Gang Liu, MD¹, Gui-Yang Xiao, MM², Chang Zhao, MD³, Yu-Cong Zou, MD¹ 

Department of ¹Rehabilitation, The third Affiliated Hospital and ³orthopedics, The Third affiliated hospital, Southern Medical University and ²Home for the Aged Guangzhou, Guangzhou, China

Objective: The current study investigated the role of CircCDR1as on angiogenesis of bone microvascular endothelial cells (BMECs) isolated from non-traumatic ONFH.

Methods: Forty corticosteroid-induced ONFH patients received THA were enrolled in our study. Expressions of CircCDR1as, miR-135b, and FIH-1 were detected by qRT-PCR in affected necrosis tissue and non-affected normal tissue. Bone microvascular endothelial cells (BMEC) were isolated from six patients and treated with 0.1 mg/mL hydrocortisone to establish a GC-damaged model of BMECs. Circ CDR1as plasmid and miR-135b mimic were transfected into BMECs. BMEC proliferation was assessed using MTT assays. The migration ability of cells was detected by scratch-wound assays. Matrigel assay was performed to detect angiogenesis *in vitro*. Western blot assay was used to detect HIF-1 α , VEGF, and FIH-1 expressions. FISH, RNA pull down, RIP, and luciferase assay were carried out to determine the interaction of CircCDR1as, miR-135b, and FIH-1.

Results: CircCDR1as was upregulated (2.02 ± 0.30 vs. 1.00 ± 0.10 , $P < 0.001$) whereas miR-135b was down-regulated (0.55 ± 0.12 vs. 1.00 ± 0.10 , $P < 0.001$) in affected tissues than in non-affected tissues. Expression of CircCDR1as and FIH-1 were negatively associated with miR-135b in affected tissues (CircCDR1as with miR-135b: $r = -0.506$, $P < 0.001$; FIH-1 with miR-135b $r = -0.510$, $P < 0.001$). Total blood tubule density was increased when CircCDR1as was silenced compared with NC ($P < 0.01$ vs. NC). The number of migrated BMECs were significantly increased in CircCDR1as silencing group compared with NC group ($P < 0.05$ vs. NC). In addition, CircCDR1as plasmids transfection increased the protein expressions of FIH-1 ($P < 0.05$ vs. NC) and reduced the HIF-1 α as well as VEGF expression compared with NC group ($P < 0.05$ vs. NC). FISH, RNA pull down, RIP, and luciferase assay identified that FIH-1 was a target of miR-135b and could be modulated by CircCDR1as.

Conclusion: CircCDR1as decreases angiogenesis and proliferation of BMECs by sponging miR-135b and upregulate FIH-1.

Key words: Non-traumatic osteonecrosis of femoral head; Bone microvascular endothelial cells; Competing endogenous RNAs; Angiogenesis

Introduction

Non-traumatic osteonecrosis of the femoral head is a progressive pathological disease that results in osteonecrosis and collapse due to the blocked blood supply of the femoral head, the interruption of local circulation, and the

impairment of the blood supply to the subchondral bone, ultimately leading to impaired hip function and permanent disability¹. It is estimated that non-traumatic ONFH cases were 8.12 mn among Chinese people aged 15 years and over². Among patients who were diagnosed with non-

Address for correspondence Yu-Cong Zou, Department of Rehabilitation, The third Affiliated Hospital, Southern Medical University, Zhong Shan Road West No.183, TianHe District, Guang Zhou, GuangDong Province, 510630, China. Tel: +86-020-62784605; Fax: +86-020-62784601; Email: zyc0118@smu.edu.cn

Received 24 August 2020; accepted 26 October 2020

traumatic ONFH, 26.35% of males and 55.75% of females reported a history of GC use³. In recent years, researchers have proposed several potential mechanisms for the development of GC-induced ONFH, including apoptosis of osteocytes and osteoblasts, increased intraosseous pressure in bone marrow adipocytes, intraosseous microvascular thrombosis, and injury of endothelial cells, etc³. Among those hypotheses, vascular hypothesis seems to be the most compelling one. This hypothesis presumes that damaged vessels and decreased local blood flow in the femoral head plays a pivotal role in the pathogenesis of ONFH^{4,5}. GC could decrease the number of blood vessels, reduce blood supply in the femoral head, and cause osteonecrosis^{6,7}. BMECs obtained from GC-induced ONFH patients have decreased angiogenic and increased apoptotic activities⁸.

Hypoxia inducible factor-1 α (HIF-1 α) is a crucial mediator of the adaptive cell response to hypoxia. It plays an important role in angiogenesis–osteogenesis coupling during bone regeneration and a protective role during ONFH⁹. Previous studies reported that HIF-1 α transfection enhanced the capability of BMCs to promote osteogenesis and angiogenesis *in vitro*^{10,11}. Ding found transplantation of HIF-1 α transgenic BMCs into the necrotic area of the femoral head could promote the repair of the necrotic tissues in a rabbit model with early-stage GC-induced ONFH¹². On the other hand, Factor Inhibiting Hypoxia Inducible Factor 1 (FIH-1), presently identified as an asparagine hydroxylase¹³, specifically hydroxylates the transcription factor HIF-1 α under normal physiological conditions and inhibits its association with the adaptor protein p300¹⁴. FIH-1 protein is widely expressed in human tissues and is thus potentially available for the regulation of HIF activity across a broad range of cells and culture conditions¹⁵. It is also suggested that FIH-1 has important non-redundant effects *in vivo* on the expression of a range of HIF transcriptional targets in normoxia and even in hypoxia¹⁶.

Circular RNAs (circRNAs), a covalently-bonded RNA transcript from back-splicing of linear RNA derived from precursor mRNA, are considered as the novel regulator in human disease¹⁷. Since circular RNAs are back-splicing products and covalently closed transcripts, they are more stable and resistant to decay machineries¹⁸. miRNAs are a class of non-coding RNA that contain ~20 nucleotides and bind to the 3'-untranslated region of mRNAs to inhibit their translation¹⁹. Emerging evidences demonstrated that circRNA take part in the pathological initiation and progression of vascular ECs by acting as aggressive endogenous RNAs that compete for miRNA-binding sites. For example, the mostly studied circRNA and circHIPK3 could inhibit the HG-induced endothelial cell apoptosis through sponging miR-124²⁰. In α LDL induced HUVECs, hsa_circ_0003575 is found to be markedly increased to regulate proliferation and apoptosis through the circRNA-miRNA-mRNA network²¹.

Accruing evidence demonstrates that CircRNA antisense to cerebellar degeneration-related protein 1 transcript (CircCDR1as) played an important role in various diseases

including cancer²², bone disease²³, and metabolism disease²⁴, etc. Recent studies suggest CircCDR1as may be involved in the development of non-traumatic ONFH. One recent study showed that CircCDR1as could promote adipogenic and suppresses osteogenic differentiation of BMSCs in steroid-induced ONFH²⁵, implicating that CircCDR1as could affect fat and bone metabolism in ONFH. However, whether CircCDR1as could affect angiogenesis of BMECs in ONFH has not been investigated yet.

Therefore, we hypothesized that: (i) expressions of CircCDR1as, miR-135b, and FIH-1 are changed in affected tissues than in non-affected tissues in non-traumatic ONFH patients; (ii) CircCDR1as is involved in angiogenesis and migration of isolated BMECs; (iii) CircCDR1as acts as a sponge of miR-135b to facilitate FIH-1 expression.

Materials and Methods

Ethics Statement

This study was approved by the Ethics Committee of the local hospital and conformed to the Helsinki Declaration. All patients signed informed consent forms.

Glucocorticoid-Damaged BMEC Model

The third generation cells of six ONFH patients were selected to establish GC-damaged BMEC model. When the cells reached about 80% confluence, hydrocortisone (Tianjin Kingyork, Tianjin, China) was introduced to the culture medium of the experimental groups, and the final concentration was 0.1 mg/mL and 0.3 mg/mL. Hydrocortisone was not added to the control group. After 24 h, the total RNAs of cell samples were extracted with TRIzol reagent (Invitrogen, Germany).

qRT-PCR

TRIzol reagent was used to extract total RNA from the obtained tissues. Thereafter, reverse transcription into cDNA was performed according to the manufacturer's protocol. The PCR amplification was done in 96-well plates. The conditions of the PCR reaction were the following: 95°C for 10 min, and amplification for 40 cycles at 95°C for 15 s and 60°C for 60 s. The specific PCR primers were as follows: CDR1as-forward: 5'-CGTCTTCCAGCATCTCTGTGT-3' and reverse: 5'-GCCATCGGAAACCCTGGATA-3'; FIH-1-forward: 5'-GCAAGGTAGGTATTCTCACTTA-3' and reverse: 5'-AAGAAC TTTCACCCTG -3'; GAPDH-forward: 5'-AATCCCATC ACCATCTTCC-3' and reverse: 5'-CATCACGCCACAG TTTCC-3'; hsa-miR-135b-forward: 5'-CGGGCTATGGCTTT TTATTCC-3', and reverse: 5'-CAGCCACAAAAGAGCAC AAT-3'; U6-forward: 5'-TGTTCCACACTACGCAGTCC-3'; U6-reverse: 5'-TTTGTCGTTCCCGTCTCCTG-3'. Expressions of CDR1as and FIH-1 were normalized to GAPDH whereas miR-135b was normalized to U6. The experiment was repeated three times to get the average value.

Cell Transfection

Cells were seeded into six-well plates at a density of 6×10^4 cells/2 ml/well and maintained in an incubator at 37 °C, 5% CO₂. When the cells reached about 80% confluency, cell transfection was performed. pcDNA3-CDR1as and its negative control (which had an inserted CDR1as sequence only but no invert repeat flanking introns into the pcDNA3.1-empty plasmid, resulting in no circular CDR1as), si-CDR1as, were conducted by GenePharma (Shanghai, China). miR-135b mimics or negative control was purchased from RiboBio (Guangzhou, People's Republic of China). BMECs were transfected with plasmids or oligonucleotides using Lipofectamine™ 2000 (Life Technologies, Carlsbad, CA, USA), according to the manufacturer's instructions. After 24 h of transfection, the efficiency of transfection was determined by qRT-PCR.

MTT Assay

To assess proliferation, BMEC cells were cultured at a concentration of approximately 1×10^4 cells per well in 96-well plates. These cells were then treated in different ways. First, 0.5% 3–4,5-dimethylthiazol-2-yl-2,5-diphenyl-tetrazolium bromide (MTT) was added to each well and incubated for 4 h at 37°C. Subsequently, 150 µl of dimethyl sulfoxide (DMSO) was added to each well. The absorbance was detected at 490 nm using a spectrophotometer.

Scratch-wound Assay

The BMEC cells cultured in six-well plates were scratched with pipette tips, and the ablated cells were washed away with phosphate-buffered saline (PBS). The cells were photographed in the same area of the culture plate at 0 h and 48 h after wounding. The mobility of the cells was determined by measuring the wound width. Migration width (%) = $(W_0 - W_{48}) / W_0 \times 100$, where W_0 is the width of the initial wound, and W_{48} is the width of the remaining wound after 48 h.

Apoptosis Assay

FITC Annexin V/Dead Cell Apoptosis Kit (Invitrogen, Shanghai, China) was used to detect the apoptosis of the cells. In brief, human BMEC cells were harvested, carefully rinsed twice using PBS and suspended in binding buffer. Next, five µL FITC Annexin V kits and one µL propidium iodide (PI) solution (100 µg/mL) were used to stain the cells (100 µL of cell suspension) for 30 min at room temperature in the dark. Then the cell apoptosis was detected by flow cytometry (Becton, Dickinson, Mountain View, USA).

In vitro Angiogenesis Assay

BMECs were cultured in endothelial cell growth medium (EGM-2) containing 10% FBS. Next, 20 µL BD Matrigel™ Matrix was diluted using serum-free RPMI-1640 medium (total amount of 40 µL) at a ratio of 1:1, which was then added into the upper surface of polyester film in the Transwell chamber (membrane well size of 8 µm) and dried in a fume hood at room temperature for 1 h. Subsequently,

200 µL cell suspension (2×10^5 cells/mL) was loaded to the apical chamber. After 24 h of incubation in a 37°C wet incubator with 5% CO₂, the branch nodes of the pseudo-tubule-like and end-to-end tubular structure formed in BMECs were observed in five randomly selected visual fields and numbered under an optical microscope.

Western Blotting

Cells were lysed using RIPA buffer and total protein was extracted from the lysate. Total protein concentration was determined using a bicinchoninic acid assay kit (KeyGen, Nanjing, China). Protein samples were separated by electrophoresis on a 13% sodium dodecyl sulfate–polyacrylamide gel and transferred to a polyvinylidene fluoride membrane (Millipore, Billerica, MA, USA). After blocking with 5% skim milk at 25°C for 1 h, the membrane was incubated with the following primary antibodies: anti-HIF-1 α (1:1000; Abcam, UK), anti-FIH-1 (1:1000; Abcam), anti-VEGF (1:1000; Beyotime, China), anti-GAPDH (1:1000; Beyotime, China). After washing with Tris-buffered saline containing 0.1% Tween 20 (TBST), the membrane was incubated with horseradish peroxidase-labeled secondary antibody IgG (1:1000; Abcam, UK) for 1 h at 37 °C. Blots were visualized with an enhanced chemiluminescence kit (Amersham, Little Chalfont, UK) and quantified using the Image Pro-Plus 6.0 analysis system (Media Cybernetics, Rockville, MD, USA). Band density values were normalized to GAPDH.

Dual-luciferase Reporter Gene Assay

The binding sites among CircCDR1AS, FIH-1, and miR-135b was predicted using bioinformatics analysis. Dual-luciferase reporter gene assay was used to verify the predicted relationship. Complementary sequence mutation sites of seed sequences were designed on the CircCDR1as-WT and FIH-1-WT, respectively. The correctly sequenced luciferase reporter plasmids WT and MUT were co-transfected with mimic NC and miR-135b mimic into BMEC cells. After 24 h of transfection, the cells were collected and lysed, followed by centrifugation at 12,000 rpm for 1 min and the collection of supernatant. The luciferase activity was determined using Dual-Luciferase® Reporter Assay System (E1910, Promega, USA). The relative luciferase (RLU) activity was calculated as the RLU activity of renilla luciferase/RLU activity of firefly luciferase. The experiment was repeated three times independently.

Fluorescence In situ Hybridization (FISH) Assay

FISH was performed using specific probes of CircCDR1as and miR-135b. The FAM-labeled probe was specific for CircCDR1as while the cy5-labeled probe was specific for miR-135b. The slides were rinsed with PBS, fixed with 4% paraformaldehyde at room temperature, treated with protease K (RNA enzyme treatment was carried out in the control experiment to verify the specificity of the signal), and hybridized in pre-hybridizing solution with probe at 42°C overnight. After PBS containing 0.1% Tween-20 (PBST) washing,

the nucleus was stained with 4', 6-diamidino-2-phenylindole (DAPI) staining solution (1:800, Thermo Fisher Scientific, Rockford, IL, USA) for 5 min, followed by three washes using PBST (3 min/time). The slides were sealed with anti-fade mounting medium, then photographed and observed in five randomly selected visual fields under a fluorescence microscope (Olympus Optical Co., Ltd., Tokyo, Japan). All images were acquired on a Zeiss LSM880 NLO confocal microscope system (Leica Microsystems, Wetzlar, Germany).

RNA Pull-Down Assay

The cells were treated with 50 nM biotin-labeled wild type (WT)-bio-miR-135b and mutation (MUT)-bio-miR-135b. After 48 h of transfection, the cells were incubated in specific lysis buffer (radioimmunoprecipitation assay [RIPA] + phenylmethylsulphonyl fluoride [PMSF] + phosphatase inhibitor = 100:1:1; Ambion Company, Austin, TX, USA) for 10 min. M-280 streptavidin magnetic beads (S3762, Sigma-Aldrich, St. Louis, MO, USA) were pre-coated with RNase-free bovine serum albumin and yeast tRNA (TRNABAK-RO, Sigma-Aldrich, St. Louis, MO, USA) and used to treat cell lysate. The bound RNA was purified by Trizol and then qPCR was performed to examine the expression CircCDR1AS. The expression of miR-135b was detected using a similar process.

RNA Binding Protein Immunoprecipitation (RIP) Assay

The binding of CircCDR1AS, miR-135b, and Argonaute2 (Ago2) was analyzed using the RIP kit (Millipore, Billerica, MA, USA). In short, the cells were washed using pre-cooled PBS and the supernatant was discarded. The cells were then lysed using lysis buffer (25 mM Tris-HCl pH 7.4, 150 mM NaCl, 0.5% Nonidet P [NP]-40, 2 mM ethylenediaminetetraacetic acid [EDTA], 1 mM NaF, 0.5 mM dithiothreitol) comprised of RNasin (Takara Biotechnology Ltd., Dalian, Liaoning, China) and protease inhibitor mixture (B14001a, Roche, Basel, Switzerland), followed by centrifugation at 12,000 g for 30 min, with the supernatant obtained. Next, a portion of cell extract was taken out as input and a portion was incubated with antibody for co-precipitation. In brief, 50 μ L magnetic beads of each co-precipitation reaction system was extracted, washed, and then re-suspended in 100 μ L RIP Wash Buffer, followed by incubation with the addition of five μ g antibodies according to the grouping for binding. Subsequently, the complex of magnetic beads-antibody was re-suspended in 900 μ L RIP Wash Buffer after washing and then incubated overnight with 100 μ L cell extract at 4°C. The antibodies used in the experiment included Ago2 (ab32381, 1:50, Abcam Inc., Cambridge, UK) which was mixed evenly at room temperature for 30 min. IgG (ab109489, 1:100, Abcam Inc., Cambridge, UK) was taken as NC. RNA was then extracted from magnetic beads using Trizol and the expression of CircCDR1AS and miR-135b was assessed using RT-qPCR.

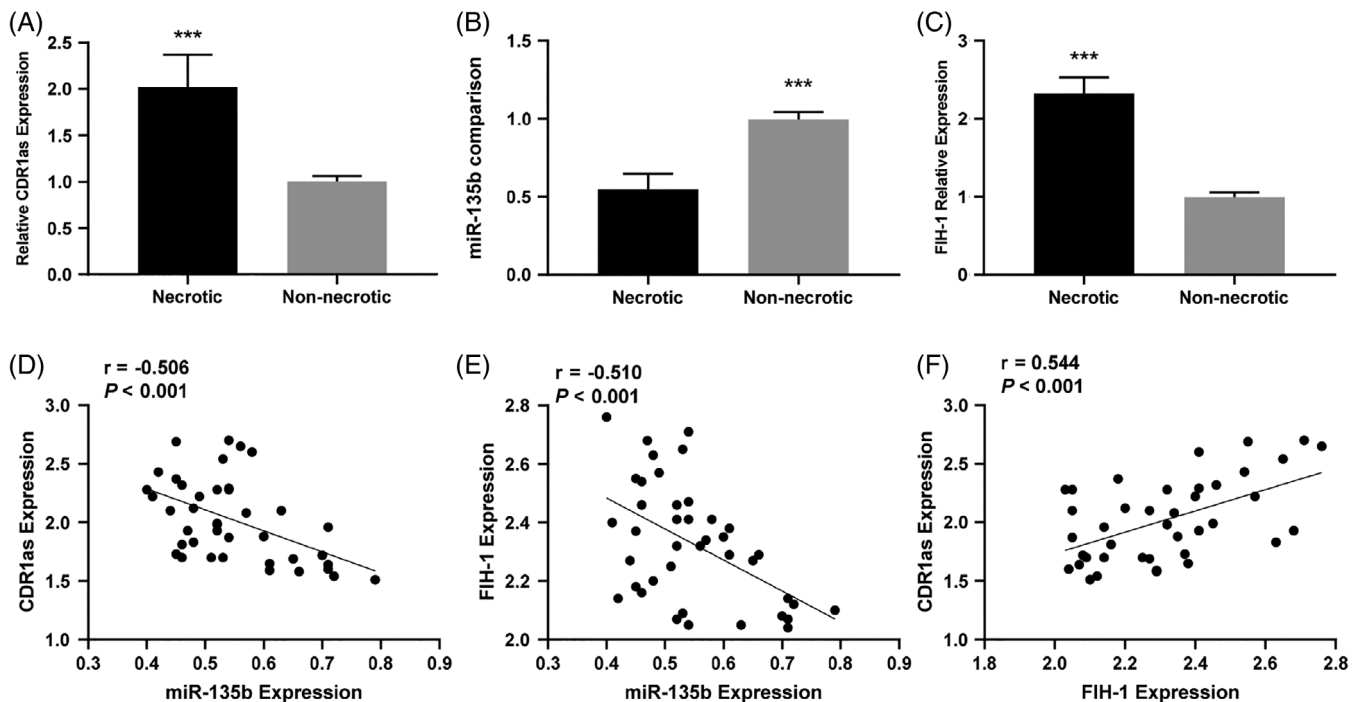


Fig. 1 (A) Comparison of local CDR1as expression between necrotic and non-necrotic tissue in ONFH patients (B) Comparison of local miR-135b expression between necrotic and non-necrotic tissue in ONFH patients (C) Comparison of FIH-1 expression between necrotic and non-necrotic tissue in ONFH patients (D) Correlation of CDR1as expression with miR-135b expression in necrotic tissue (E) Correlation of FIH-1 expression with miR-135b expression in necrotic tissue (F) Correlation of FIH-1 expression with CDR1as expression in necrotic tissue (***) $P < 0.001$.

Statistical Analysis

Obtained data were expressed as mean \pm standard deviation. Comparison between two groups with normal distribution and homogeneity of variance was analyzed using the unpaired t-test. Data within one group were analyzed using the paired t-test. Comparisons among multiple groups were analyzed by one-way analysis of variance (ANOVA), followed by Tukey's post-hoc test. Data comparison among groups at different time points was performed by repeated-measures ANOVA, followed by Bonferroni post-hoc test. A value of $P < 0.05$ was regarded as statistically significant. All data were analyzed using Graphpad prism 8.0 software.

Results

CircCDR1as and FIH-1 Expressions Were Remarkably Highly Expressed in Necrotic Tissue While miR-135b was Significantly Lowly Expressed

To explore the associations among CircCDR1as, miR-135b, and FIH-1, we firstly used qRT-PCR to detect CircCDR1as, miR-135b, and FIH-1 mRNA expressions, respectively, in necrotic tissues and adjacent non-necrotic tissues of non-

traumatic ONFH patients. The results suggested that compared with that of non-necrotic tissues, the expressions of CircCDR1as and FIH-1 in necrotic tissue were significantly up-regulated, while miR-135b expression was down-regulated ($***P < 0.001$, Fig. 1A–C). Correlation analysis was then performed and revealed a negative correlation between CircCDR1as and miR-135b ($r = -0.506$, $P < 0.001$, Fig. 1D); FIH-1 and miR-135b expressions were also negatively correlated ($r = -0.510$, $P < 0.001$, Fig. 1E), while CircCDR1as expression and FIH-1 expression were positively correlated ($r = 0.544$, $P < 0.001$, Fig. 1F). These data implied potential regulatory relationships among CircCDR1as, miR-135b, and FIH-1.

CircCDR1as Knockdown Alleviated Apoptosis and Enhanced Cell Viability of BMECs

We next carried out MTT assay as well as flow cytometry analysis to test the cell viability and apoptosis. MTT assay indicated that CircCDR1as overexpression decreased the proliferative ability of BMECs, while CircCDR1as knockdown recovered the proliferation compared with controls. Co-transfection of CircCDR1as with miR-135b mimic had

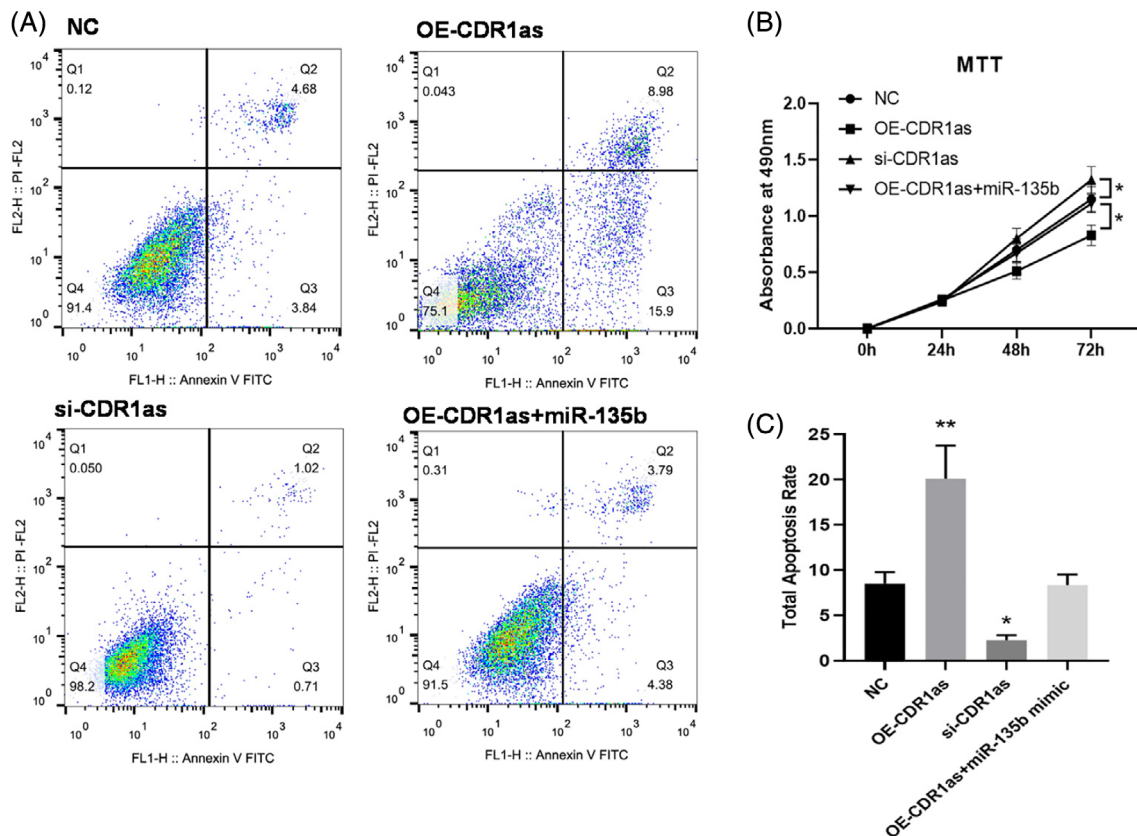


Fig. 2 (A) At 48 h after transfection, BMECs were stained with Annexin V-FITC and PI, and the cell apoptosis rate was evaluated by flow cytometry (B) Following transfection with OE-CDR1as, si-CDR1as, and OE-CDR1as + miR-135b, the cellular proliferation of BMECs was assessed by an MTT assay. $*P < 0.05$ vs. NC (C) The histogram of total cell apoptosis rate. $*P < 0.05$; $**P < 0.01$ vs. NC.

similar cell viability with NC group (Fig. 2B). In addition, we found that CircCDR1as knockdown alleviated BMECs apoptosis. On the other hand, CircCDR1as overexpression promoted BMECs apoptosis. Co-transfection of CircCDR1as with miR-135b mimic had the similar cell apoptosis rate with NC group (Fig. 2A,C).

Downregulation of CircCDR1as Promoted Angiogenesis and Migration of BMECs

The effects of CircCDR1as on BMECs blood tubule formation (48 h) were evaluated. Specifically, total tubule density was increased when CircCDR1as was silenced compared with NC. On the other hand, the total tubule density decreased when CircCDR1as was overexpressed, and adding miR-135b mimic could reverse this condition (Fig. 3B,D).

We next performed wound-healing assay to discuss whether CircCDR1as could affect migration of BMECs at 48 h. The number of migrated BMECs were significantly increased in CircCDR1as silencing group compared with NC group, whereas a markedly decreased migrated BMECs was observed in CircCDR1as overexpression group. Co-transfection of CircCDR1as and miR-135b mimic had

similar number of migrated BMECs compared with NC group (Fig. 3C).

FIH-1 was a Target of miR-135b and Could be Modulated by CircCDR1as

To fathom the potential mechanism of CircCDR1as /miR-135b/FIH-1 axis, the target genes of miR-135b was predicted by multiple online bioinformatics databases (http://www.targetscan.org/vert_72/; <http://www.microrna.org/microrna/home.do>; <http://mirdb.org/miRDB/>), and it showed that FIH-1 and CircCDR1as had the potential to be a target of miR-135b (Fig. 4A,B). Subsequently, dual luciferase reporter experiments revealed that miR-135b specifically bound to the 3'UTR of FIH-1 and CircCDR1as ($P < 0.05$, Fig. 4C,D). Furthermore, findings concluded by FISH, RIP, and RNA pull-down assay suggested the FIH-1, CircCDR1as, and miR-135b were directly interacted (Fig. 4E-H).

Silencing CircCDR1as Increased Protein Expressions of VEGF as Well as HIF-1 α and Decreased FIH-1 Expressions

We last examined whether CircCDR1as could affect VEGF, HIF-1 α , and FIH-1 protein expressions. We found

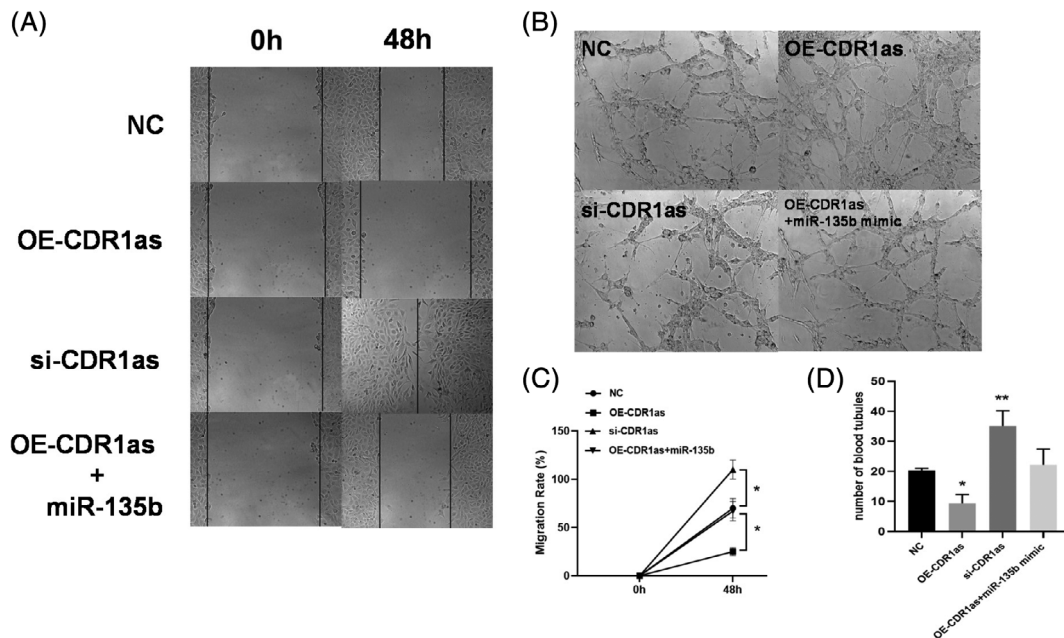


Fig. 3 Effects of CircCDR1as on the migration and angiogenesis of BMECs. (A) Representative images of wound scratch-wound assays after transfecting bone microvascular endothelial cells (BMECs) with CDR1as, si-CDR1as, OE-CDR1as + miR-135b, and NC. Images were taken at 0 and 48 h after the cell layer was scratched with a pipette tip. Scale bar: 50 μ m. (B) Representative images of tube formation assays at 48 h after seeding BMECs transfected with OE-CDR1as, si-CDR1as, OE-CDR1as + miR-135b, and NC on Matrigel. Scale bar: 100 μ m. (C) Statistical analysis of the wound-healing rates revealed that transfection with OE-CDR1as statistically significantly inhibited BMEC migration compared with that of the NC group whereas transfecting si-CDR1as had the opposed effect. (D) Statistical analysis of the relative change in tube length revealed that transfection with OE-CDR1as had statistically significantly inhibited tube formation in BMECs compared with that of the NC group, whereas transfecting si-CDR1as had the opposed effect. $n = 3$ per group. * $P < 0.05$, ** $P < 0.01$.

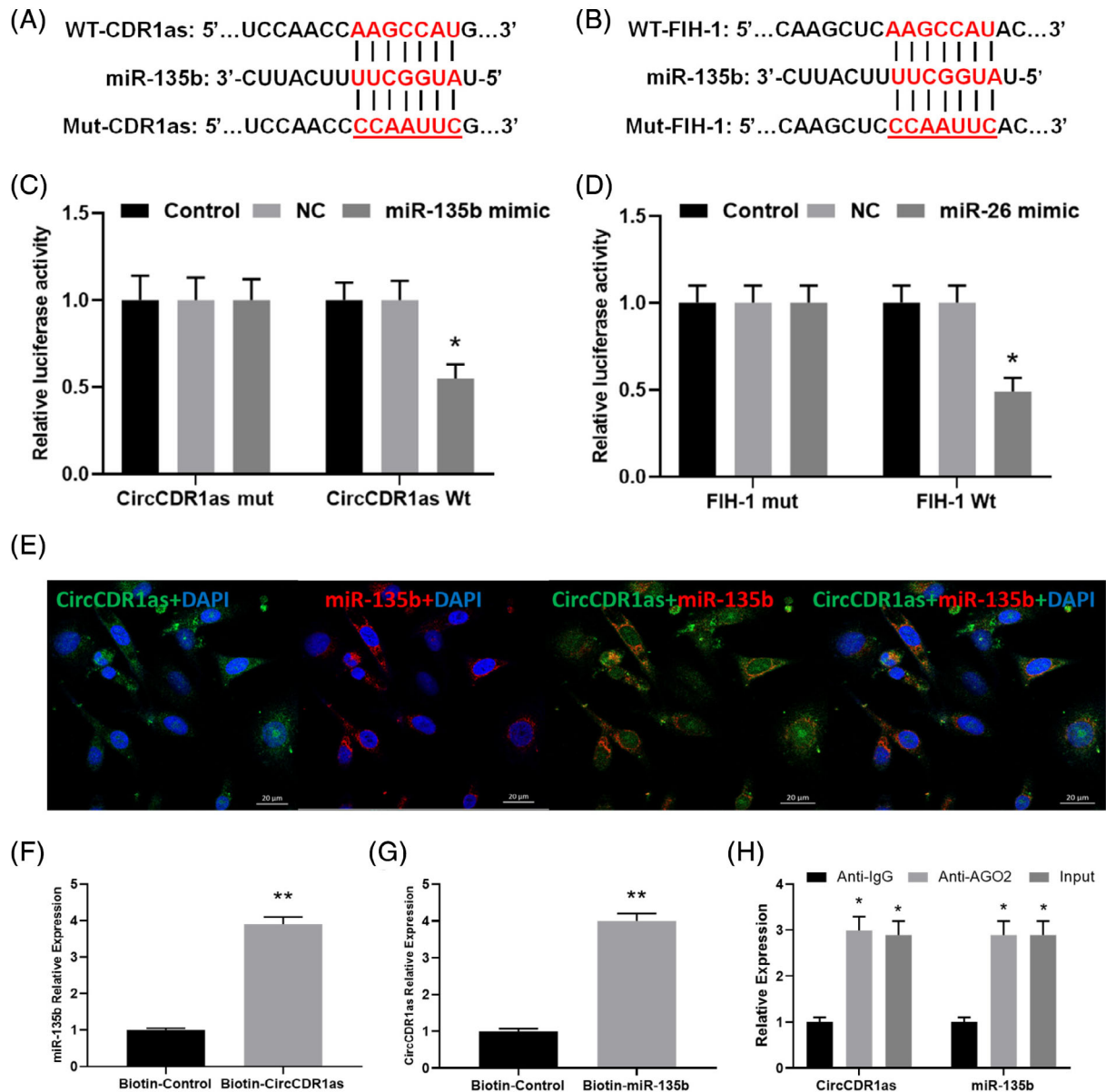


Fig. 4 (A, B) miR-135b directly binds to CircCDR1as and FIH-1. Two different types of luciferase reporter vectors were constructed: wild-type CircCDR1as and FIH-1 3'UTR, and mutant-type CircCDR1as and FIH-1 3'UTR. (C, D) The above vectors were co-transfected into BMECs with miR-135b mimics or NC and examined for luciferase activity (* $P < 0.05$). (E) CircCDR1as and miR-135b were colocalized in BMECs by FISH using confocal microscope. miR-135b was stained red, CircCDR1as was stained green, nuclei were stained blue (DAPI) and overlapped expression was mixed (Scale bar, 20 μm). (F) The biotin-coupled probe pull-down assay was performed and the results showed miR-135b was detected in the CircCDR1as pulled-down pellet compared with the control group. (G) CircCDR1as was detected in the biotin-miR-135b vector compared with the control group. (H) CircCDR1as and miR-135b expression presented as fold enrichment in Ago2 relative to normal IgG immunoprecipitates. RIP assays disclosed that CircCDR1as and miR-135b expressions were substantially enriched by Ago2 antibody compared with control IgG antibody.

pcDNA3-CDR1as transfection increased the protein expression of FIH-1 and decreased VEGF as well as HIF-1 α expressions compared with NC. On the other hand, knockdown of CircCDR1as downregulated FIH-1 protein expression and upregulated VEGF as well as HIF-1 α expressions than that in NC. Co-transfection of pcDNA3-CDR1as and miR-135b

mimic had no significant differences with regard to these protein expressions compared with NC, indicating the function of OE-CircCDR1as was attenuated by miR-135b in BMECs (Fig. 5A–D). These data demonstrated that CircCDR1as/miR-135b/FIH-1 axis may influence the process of BMECs angiogenesis.

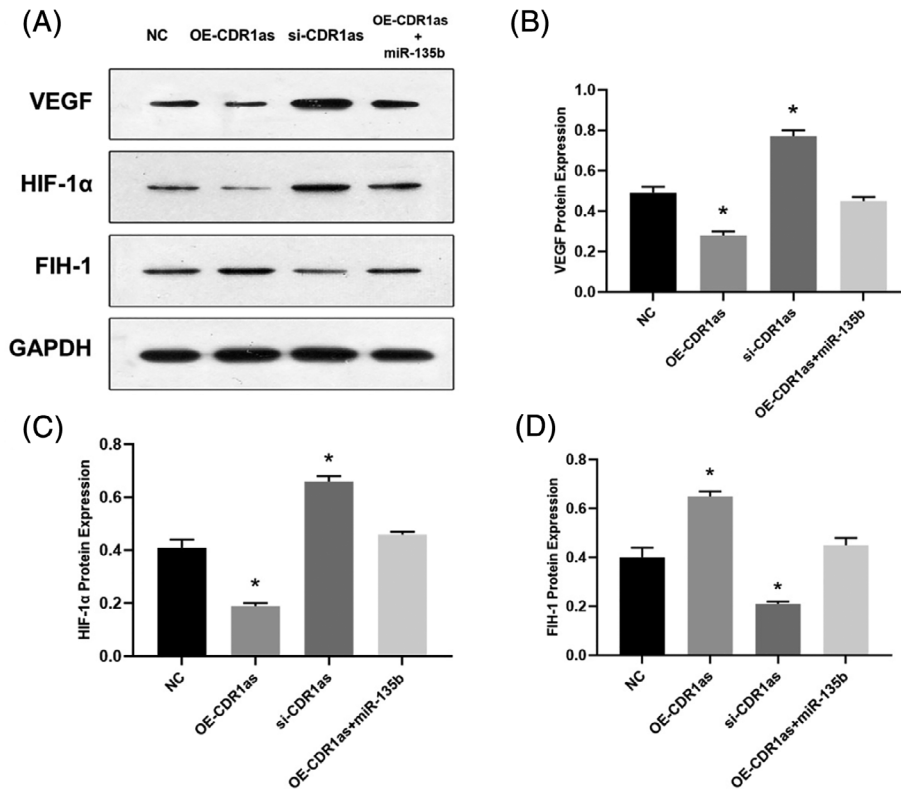


Fig. 5 Western Blot analysis (A) of VEGF (B), HIF-1α (C), FIH-1 (D) followed by CircCDR1as transfection (* $P < 0.05$ vs. NC).

Discussion

The current study investigated the potential role of CircCDR1as regulating miR-135b/FIH-1 axis in the angiogenesis ability in isolated BMECs. CircCDR1as was upregulated whereas miR-135b was downregulated more in affected tissues than in non-affected tissues. Overexpression of Circ CDR1as inhibited BMEC proliferation, migration rate, and impaired angiogenesis ability whereas adding miR-135b could rescue these conditions. In addition, Circ CDR1as plasmids transfection increased the protein expressions of FIH-1 and reduced the HIF-1α as well as VEGF expression. FISH, RNA pull down, RIP, and luciferase assay identified that Circ CDR1as acts as a sponge of miR-135b to facilitate FIH-1 expression. These findings implicated that CircCDR1as may inhibit angiogenesis of BMECs through miR-135b/FIH-1 axis.

Endothelial cell damage, intravascular coagulation, and disordered angiogenesis result in ischemia, which is regarded as the core pathological results of ONFH⁶. Endothelial cell tube formation is the first step in neovascularization²⁶, and blood vessels are critical in bone remodeling because they supply nutrients²⁷. It has been reported that steroid-induced ONFH may cause miRNA alterations in femoral head bone microvascular endothelial cells that are not seen in controls²⁸. The vascularity of the bone in osteonecrosis is reduced by almost 50%²⁷. Additionally, a reduction in bone strength and vascularity of the bone precedes bone mass reduction and microstructural deterioration²⁹. Previous studies have suggested that ameliorating vascular endothelial cell

proliferation, migration, and tube formation may positively promote bone vascularization in the femoral head and prevent ONFH^{30,31}.

Recently, CircRNAs have been proven to be expressed in endothelial cells and exert a biological effect in angiogenesis³². For example, circRNA 0003575 is upregulated in oxidized low-density lipoprotein-induced human umbilical vein endothelial cells (HUVECs), and promotes HUVEC proliferation and angiogenesis²¹. CircRNA 0010729 mediates vascular endothelial cell apoptosis and proliferation by targeting the miR-186/hypoxia inducible factor-1α axis³³. Furthermore, Shan *et al.*³⁴ reported that circCDR1AS expression is substantially upregulated in endothelial cells during diabetic retinal vasculopathy and act as an endogenous miR-30a-3p sponge, and downregulation of circCDR1AS also attenuates retinal vascular dysfunction³⁴. Therefore, it was hypothesized that CircRNAs may be involved in the endothelial cell damage and disruption of angiogenesis that lead to the formation of ONFH and serve as potential therapeutic targets.

In the current study, we found CircCDR1as acts as a sponge of miR-135b/ FIH-1 to suppress BMECs activity and accelerate angiogenesis injury, whereas knockdown of CircCDR1as promoted angiogenesis *in vitro*. One study identified that miR-135b directly suppressed FIH-1 in endothelial cells³⁵. In our study, we found that miR-135b also targets FIH-1 in BMECs. miR-135b is an oncogenic microRNA that has been linked to the progression of various cancers³⁶,

cardiovascular diseases³⁷, and Parkinson's disease³⁸, etc. Some targets already reported the direct binding of miR-135b (such as SMAD5 and SMAD4)³⁹. To the best of our knowledge, there is no report dealing with an association between those targets and angiogenesis with regard to ONFH. Zhang *et al.* demonstrated a parallel correlation between miR-135b and HIF-1 α ; miR-135b is more involved with mechanisms of hypoxic response⁴⁰.

Furthermore, we investigated the mechanism of CircCDR1as in GC-induced ONFH. The results of FISH, RNA pull-down assay, RIP and Luciferase activity assay in our study showed that CircCDR1as directly interacted with miR-135b. Therefore, we investigated the sponge function of CircCDR1as. According to our study, CircCDR1as/miR-135b/FIH-1 may be a cascade to regulate angiogenesis in GC-induced ONFH. Previous studies showed the CircCDR1as could regulate the proliferation and apoptosis of human cardiomyocytes partially through -135b/HMOX1 axis⁴¹. Another study demonstrated that CircCDR1as acts as a sponge of miR-135b-5p to suppress ovarian cancer progression⁴². In our study, CircCDR1as as a sponge of miR-135b regulated the angiogenesis effect in GC-induced by targeting FIH-1. Overexpressed CircCDR1as can downregulate

the expression of FIH-1. The results of our study also demonstrated that CircCDR1as downregulated the angiogenesis marker including VEGF and HIF-1 α .

There were some limitations that should be taken into account. First of all, this study is carried out using isolated BMECs, further animal models are needed for discussing the potential mechanisms of CircCDR1as in the development of non-traumatic ONFH. Second, we only explored CircCDR1as in this study, investigation of other potential non-coding RNAs may reveal more valuable information.

In short, our study demonstrated that the enhancing of CircCDR1as could downregulate the expression of miR-135b and down-regulate the expression of FIH-1, thus enhancing the proliferation and angiogenesis ability of BMECs. Collectively, these findings suggested that CircCDR1as could increase the expression of FIH-1 by binding to miR-135b, highlighting the potential detrimental contribution of CircCDR1as to non-traumatic ONFH. The present study provides new insights for the clinical therapy of non-traumatic ONFH. However, more in-depth investigation underlying the potential regulatory pathway of CircCDR1as/HIF-1 α /FIH-1 is required in the future.

References

- di Benedetto P, Niccoli G, Beltrame A, *et al.* Histopathological aspects and staging systems in non-traumatic femoral head osteonecrosis: an overview of the literature. *Acta Bio-Medica*, 2016, 87: 15–24.
- Zhao DW, Yu M, Hu K, *et al.* Prevalence of nontraumatic osteonecrosis of the femoral head and its associated risk factors in the Chinese population: results from a nationally representative survey. *Chin Med*, 2015, 128: 2843–2850.
- Nishimura T, Matsumoto T, Nishino M, Tomita K. Histopathologic study of veins in steroid treated rabbits. *Clin Orthop Relat Res*, 1997, 334: 37–42.
- Kerachian MA, Harvey EJ, Courmoyer D, Chow TY, Seguin C. Avascular necrosis of the femoral head: vascular hypotheses. *Endothelium*, 2006, 13: 237–244.
- Jacobs B. Epidemiology of traumatic and nontraumatic osteonecrosis. *Clin Orthop Relat Res*, 1978, 130: 51–67.
- Kerachian MA, Seguin C, Harvey EJ. Glucocorticoids in osteonecrosis of the femoral head: a new understanding of the mechanisms of action. *J Steroid Biochem Mol Biol*, 2009, 114: 121–128.
- Zhang Q, LVJ JL. Role of coagulopathy in glucocorticoid-induced osteonecrosis of the femoral head. *J Int Med Res*, 2018, 46: 2141–2148.
- Yu H, Liu P, Zuo W, *et al.* Decreased angiogenic and increased apoptotic activities of bone microvascular endothelial cells in patients with glucocorticoid-induced osteonecrosis of the femoral head. *BMC Musculoskelet Disord*, 2020, 21: 1.
- Riddle RC, Khatri R, Schipani E, *et al.* Role of hypoxia-inducible factor-1 α in angiogenic-osteogenic coupling. *J Mol Med (Berl)*, 2009, 87: 583–590.
- Zou D, Han W, You S, *et al.* In vitro study of enhanced osteogenesis induced by HIF-1 α -transduced bone marrow stem cells. *Cell Prolif*, 2011, 44: 234–243.
- Keith B, Simon MC. Hypoxia-inducible factors, stem cells, and cancer. *Cell*, 2007, 129: 465–472.
- Ding H, Gao YS, Hu C, *et al.* HIF-1 α transgenic bone marrow cells can promote tissue repair in cases of corticosteroid-induced osteonecrosis of the femoral head in rabbits. *PLoS One*, 2013, 8: e63628.
- Koivunen P, Hirsila M, Gunzler V, *et al.* Catalytic properties of the asparaginyl hydroxylase (FIH) in the oxygen sensing pathway are distinct from those of its prolyl 4-hydroxylases. *J Biol Chem*, 2004, 279: 9899–9904.
- Mahon PC, Hirota K, Semenza GL. FIH-1: a novel protein that interacts with HIF-1 α and VHL to mediate repression of HIF-1 transcriptional activity. *Genes Dev*, 2001, 15: 2675–2686.
- Elkins JM, Hewitson KS, McNeill LA, *et al.* Structure of factor-inhibiting hypoxia-inducible factor (HIF) reveals mechanism of oxidative modification of HIF-1 α . *J Biol Chem*, 2003, 278: 1802–1806.
- Stolze IP, Tian YM, Appelhoff RJ, *et al.* Genetic analysis of the role of the asparaginyl hydroxylase factor inhibiting hypoxia-inducible factor (HIF) in regulating HIF transcriptional target genes. *J Biol Chem*, 2004, 279: 42719–42725.
- Wu J, Qi X, Liu L, *et al.* Emerging epigenetic regulation of circular RNAs in human cancer. *Mol Ther Nucleic Acids*, 2019, 16: 589–596.
- Li X, Yang L, Chen LL. The biogenesis, functions, and challenges of circular RNAs. *Mol Cell*, 2018, 71: 428–442.
- Bartel DP. MicroRNAs: target recognition and regulatory functions. *Cell*, 2009, 136: 215–233.
- Cao Y, Yuan G, Zhang Y, Lu R. High glucose-induced circHIPK3 downregulation mediates endothelial cell injury. *Biochem Biophys Res Commun*, 2018, 507: 362–368.
- Li CY, Ma L, Yu B. Circular RNA hsa_circ_0003575 regulates oxLDL induced vascular endothelial cells proliferation and angiogenesis. *Biomed Pharmacother*, 2017, 95: 1514–1519.
- Yu L, Gong X, Sun L, Zhou Q, Lu B, Zhu L. The circular RNA Cdr1as act as an oncogene in hepatocellular carcinoma through targeting miR-7 expression. *PLoS One*, 2016, 11: e0158347.
- Zhang W, Zhang C, Hu C, Luo C, Zhong B, Yu X. Circular RNA-CDR1as acts as the sponge of microRNA-641 to promote osteoarthritis progression. *J Inflamm (Lond)*, 2020, 17: 8.
- Xu H, Guo S, Li W, Yu P. The circular RNA Cdr1as, via miR-7 and its targets, regulates insulin transcription and secretion in islet cells. *Sci Rep*, 2015, 5: 12453.
- Chen G, Wang Q, Li Z, *et al.* Circular RNA CDR1as promotes adipogenic and suppresses osteogenic differentiation of BMSCs in steroid-induced osteonecrosis of the femoral head. *Bone*, 2020, 133: 115258.
- Carulli C, Innocenti M, Brandi ML. Bone vascularization in normal and disease conditions. *Front Endocrinol (Lausanne)*, 2013, 4: 106.
- Lane NE. Glucocorticoid-induced osteoporosis: new insights into the pathophysiology and treatments. *Curr Osteoporos Rep*, 2019, 17: 1–7.
- Yue J, Wan F, Zhang Q, *et al.* Effect of glucocorticoids on miRNA expression spectrum of rat femoral head microcirculation endothelial cells. *Gene*, 2018, 651: 126–133.
- Weinstein RS, Hogan EA, Borrelli MJ, Liachenko S, O'Brien CA, Manolagas SC. The pathophysiological sequence of glucocorticoid-induced osteonecrosis of the femoral head in male mice. *Endocrinology*, 2017, 158: 3817–3831.
- Liu X, Li Q, Niu X, *et al.* Exosomes secreted from human-induced pluripotent stem cell-derived mesenchymal stem cells prevent osteonecrosis of the femoral head by promoting angiogenesis. *Int J Biol Sci*, 2017, 13: 232–244.
- Zhang Y, Yin J, Ding H, Zhang C, Gao YS. Vitamin K2 ameliorates damage of blood vessels by glucocorticoid: a potential mechanism for its protective effects in glucocorticoid-induced osteonecrosis of the femoral head in a rat model. *Int J Biol Sci*, 2016, 12: 776–785.
- Boeckel JN, Jaé N, Heumüller AW, *et al.* Identification and characterization of hypoxia-regulated endothelial circular RNA. *Circ Res*, 2015, 117: 884–890.
- Dang RY, Liu FL, Li Y. Circular RNA hsa_circ_0010729 regulates vascular endothelial cell proliferation and apoptosis by targeting the miR-186/HIF-1 α axis. *Biochem Biophys Res Commun*, 2017, 490: 104–110.

- 34.** Shan K, Liu C, Liu BH, *et al.* Circular noncoding RNA CDR1AS mediates retinal vascular dysfunction in diabetes mellitus. *Circulation*, 2017, 136: 1629–1642.
- 35.** Umezumi T, Tadokoro H, Azuma K, Yoshizawa S, Ohyashiki K, Ohyashiki JH. Exosomal miR-135b shed from hypoxic multiple myeloma cells enhances angiogenesis by targeting factor-inhibiting HIF-1. *Blood*, 2014, 124: 3748–3757.
- 36.** Xin Y, Yang X, Xiao J, *et al.* MiR-135b promotes HCC tumorigenesis through a positive-feedback loop. *Biochem Biophys Res Commun.*, 2020, 530: 259–265.
- 37.** Li A, Yu Y, Ding X, *et al.* MiR-135b protects cardiomyocytes from infarction through restraining the NLRP3/caspase-1/IL-1 β pathway. *Int J Cardiol*, 2020, 307: 137–145.
- 38.** Zeng R, Luo DX, Li HP, Zhang QS, Lei SS, Chen JH. MicroRNA-135b alleviates MPP+mediated Parkinson's disease in in vitro model through suppressing FoxO1-induced NLRP3 inflammasome and pyroptosis. *J Clin Neurosci*, 2019, 65: 125–133.
- 39.** Song Z, Chen LL, Wang RF, *et al.* MicroRNA-135b inhibits odontoblast-like differentiation of human dental pulp cells by regulating Smad5 and Smad4. *Int Endod J*, 2017, 50: 685–693.
- 40.** Zhang L, Sun ZJ, Bian Y, Kulkarni AB. MicroRNA-135b acts as a tumor promoter by targeting the hypoxia-inducible factor pathway in genetically defined mouse model of head and neck squamous cell carcinoma. *Cancer Lett*, 2013, 331: 230–238.
- 41.** Chen C, Shen H, Huang Q, Li Q. The circular RNA CDR1as regulates the proliferation and apoptosis of human cardiomyocytes through the miR-135a/HMOX1 and miR-135b/HMOX1 axes. *Genet Test Mol Biomarkers*, 2020, 24: 537–548. <https://doi.org/10.1089/gtmb.2020.0034>.
- 42.** Chen H, Mao M, Jiang J, Zhu D, Li P. Circular RNA CDR1as acts as a sponge of miR-135b-5p to suppress ovarian cancer progression. *Oncotargets Ther*, 2019, 12: 3869–3879.